A Pseudogravimetric Study of Part of the Upper Benue Trough, Nigeria

Mohammed L. Garba[1], Charles O. Ofoegbu[2], Etim D. Uko[2] Samson. D. Yusuf[2]

[1]Department of General Studies, The Federal Polytechnic Bauchi Nigeria

[2]Department of Physics, Nasarawa State University Keffi Nigeria

DOI: https://doi.org/10.51584/IJRIAS.2024.909024

Received: 26 July 2024; Accepted: 10 August 2024; Published: 04 October 2024

ABSTRACT

Pseudogravimetric transform is a linear filtering procedure for converting the magnetic anomaly over a magnetization distribution into the corresponding gravity anomaly. The transformation typically eliminates the characteristic asymmetrical nature of magnetic anomalies relative to their sources and enhances the long wavelength anomalies while attenuating those with short wavelengths. This method was employed in a study of part of the Upper Benue Trough in northeastern Nigeria carried in which case a grid of the total magnetic field intensity (TMI) of the studied area was transformed into a grid of pseudogravimetric (PSG) anomaly. The Total Magnetic Intensity ranged between -172.9 nT and 195.1 nT, while the Pseudogravimetric (PSG) anomaly of the TMI ranged from -42.4 milliGal to 19.7 milliGal. Qualitative interpretation, computation of the derivatives of the pseudogravimetric (PSG) anomaly and comparisons of the grid satellite gravity data with the grid of the pseudogravimetric (PSG) data have been carried out to facilitate the understanding of the origin of the magnetic anomalies in the trough. The result of the analysis shows a correlation between the PSG anomaly and the satellite gravity data in the southern part indicating a common source probably basement igneous intrusions and a negative correlation between them in the northern part probably indicating a sedimentary section with high magnetic susceptibility within it (intra-sedimentary magnetic anomaly). The derivatives of the Pseudogravimetric (PSG) anomaly identified igneous basement intrusions, basement topography, and variable magnetic susceptibility as probable causes of the magnetic anomalies. Spectral analysis was used for quantitative interpretation, determining depths ranging from 443 m to 7.74 km.

Keywords: Pseudogravimetric transformation, Benue trough, Satellite gravity, Spectral analysis.

INTRODUCTION

The Upper Benue Trough is a part of the larger Benue Trough, a major linear SW-NE sedimentary basin located in Nigeria and formed during the rifting of the African and South American plates during the Cretaceous period. This breakup led to the opening of the Atlantic Ocean and the separation of the African and South American continents. The trough is described as an extensional graben system (Crachley & Jones, 1965) and a third failed or an aulacogen of a three-armed rift system (Wright, 1968). It has experienced complex tectonic movement, including crustal extension and thinning leading to the formation of rift system, faults, folds and flexures, volcanic intrusions and lineaments which have significantly influenced the basin's geological structure and hydrocarbon and mineral deposits potential.

The interpretation of magnetic anomaly is relatively more complex than the corresponding gravity anomaly. Firstly, the dipolar nature of the magnetic field has positive and negative parts in contrast to the simpler monopolar gravity field. Secondly, the magnetization vector of a source body is dependent upon the latitude due to the variability of the ambient field over the Earth's surface (Blakely, 1995). Also, rock total magnetization is a vector addition of both remanent and geomagnetic induced components. As a result, the shape of a magnetic anomaly relative to its source is distorted causing a decrease in the amplitude of the anomaly, asymmetry in the anomaly and a shift of the peak of the anomaly to the south in the northern geomagnetic hemisphere and the converse in the southern geomagnetic hemisphere. Furthermore, if shallow magnetic sources do exist, these are

ISSN No. 2454-6194 | DOI: 10.51584/IJRIAS |Volume IX Issue IX September 2024

usually of short wavelengths and discrete and can mask the identification of the medium and longer wavelengths, thereby complicating their interpretation (Hinze et al., 2010).

To simplify all these complexities associated with the measured magnetic anomalies, Baranov (1957), described an application of Poisson's relation in which a grid of the total magnetic field anomaly is converted into a grid of gravity effects called pseudogravity anomaly by assuming that the sources have a correlative magnetization and density variations. (i.e., $\frac{M}{\rho}$ is a constant throughout the source). The pseudogravimetric maps appear as gravity maps and are therefore free from the distortion in magnetic maps that are caused by the strike and dip of the magnetic polarization and fields. Pseudogravimetric maps are particularly useful in enhancing the regional anomalies and attenuating the residuals in a composite magnetic map. The transformation will therefore be useful in mapping deep magnetic sources in the mapped area (David & Zhikun, 2004). The transformation may also be used to investigate a possible common source of both gravity and magnetic anomalies (Ofoegbu, 1985). According to Panepinto, et al. (2014), it can be used to enrich gravity data and also makes it is possible to determine the depth to the magnetic basement (Ahmed et al., 2013; David & Zhikun, 2004).

Gravity and magnetic anomalies have been used to study the framework of the Upper Benue trough of the Benue rift system. Ofoegbu (1988) carried out an aeromagnetic study of a part of the Upper Benue tough and interpreted the anomalies in terms of intrusive bodies and the basement topology. Shemang et al. (2004), investigated the gravity anomalies over the Gongola arm of the Upper Benue Trough and interpreted the positive gravity anomalies in terms of mafic intrusives into the sediments. Salako and Udensi (2013) carried out a spectral analysis of aeromagnetic data over the Upper Benue Trough. This work aims to study a part of the Upper Benue trough, Nigeria using Pseudogravimetric transformation.

Location of Study area

The area of study is a part of the Upper Benue Trough, encompassing regions within Bauchi, Gombe and Adamawa states in northeastern Nigeria, bounded by latitude 9º.00N to11.30ºN and longitude10º.30E to 12º.00E (Figure 1.1).

Geology of Study area

The African continent is characterized by two major rift systems: the East African Rift System of Tertiary to Recent age and the West and Central African Rift System of Cretaceous to Early Tertiary age. The NE trending Benue Trough is the main component of the West and Central African Rift System. It extends for about 800km in length, 50 km -150 km in width, and is estimated to contain 5,000m of cretaceous sediments and volcanic rocks. It forms an important part of a system of linear sedimentary basins which include rivers Benue, Niger, and the Gongola (Ofoegbu, 1984).

According to Ofoegbu (1984), the evolution of the Benue trough is thought to have involved the rise of a mantle plume giving rise to up doming and development of initial lines of weaknesses marginal to the plume. Renewed mantle plume activity and up doming gave rise to the emplacement of intrusive bodies along the lines of weakness and consequently block faulting. The continued emplacement of intrusive materials enhanced the breakup of the crust and block faulting, giving rise to the rather irregular topography of the basement

The Benue Trough has for long been recognized as one of the main structures associated with the breakup of Gondwanaland, the separation of Africa from South America and the opening of the South Atlantic Ocean. It runs from the northern boundary of the Niger Delta to the Southern boundary of the Chad Basin. The Benue Trough is arbitrarily divided into three basins: Lower Benue, Middle Benue, and Upper Benue Trough. The Trough is filled with Cretaceous rocks whose ages range from Middle Albian to Maastrichtian, of which those predating the mid-Santonian have been compressional, folded, faulted, and uplifted in several places (Obaje, 2009). Compressional folding during the mid-Santonian tectonic episode affected the whole of the Benue Trough producing over 100 anticlines and synclines.

Upper Benue Trough is the northern section of the elongated Benue trough and is made up of three basins: The trending Gongola basin (Gongola arm), the east-trending Yola basin (Yola arm), and the northeast-trending Lau

ISSN No. 2454-6194 | DOI: 10.51584/IJRIAS |Volume IX Issue IX September 2024

basin (Main arm). The geology consists of crystalline basement, Cretaceous sediments, and volcanics. The Precambrian crystalline basement is made up of scattered remains of well-metamorphosed sedimentary rocks and diverse, mostly granite, plutonic masses that are collectively called older granites.

The earliest Cretaceous sequence is the continental Albian Bima (Figure 1.2) sandstone which rests uncomfortably on the undulating Precambrian basement. The Bima Sandstone is the most extensive earliest continental sediments deposited on the entire basin, northeast Nigeria as a basal unit of the Cretaceous series soon after crustal rifting The Bima sandstone is dominantly a quartz arenite derived from juxtaposed basement suites of the granites and gneisses which were subjected to humid conditions that accelerated the weathering process. From the field relationships of the beds, it is possible to differentiate the formation into lower Bima, Middle Bima, and Upper Bima.

Overlying the Bima Formation conformably is the Yolde Formation. This formation is of the Cenomanian age and represents the beginning of marine incursion into this part of the trough. It comprises of alternating sandstone and sales. The sandstones are fine to medium-grained and light brown, with shale and limestone intercalations. The base of the Yolde Formation is defined by the first appearance of the marine shale and the top by the disappearance of sandstones and the appearance of limestone-shale deposits.

Lying conformably on the Yolde formation, in the Gongola arm are the laterally equivalent Gongila and Pindiga Formations with the Dukku/Jessu formation in the Yola arm and the younger Fika shale. These formations represent full marine incursion into the Upper Benue Trough during the Turonian-Santonian times. Lithologically, these formations are characterized by the dark carbonated shales and limestones (Obaje, 2009).

Post-folding sediments are represented by the continental Gombe Formation of the Maastrichtian age and the Keri-Keri Formation of the Tertiary age. The Gombe Sandstone is lithologically like the Bima Sandstone, attesting to the re-establishment of the Albian paleoenvironmental conditions (Obaje, 2009). The Keri-Keri formation which includes Gombe, Dukku, and Alkaleri, is made up of sandstones, Shale, Coal, with sandstone dominating the lithology in most places (Figure 1.2). The region also contains volcanic rocks such as basalts, phonolites, and trachyte. These rocks are associated with the tectonic activity that has influenced the trough's evolution.

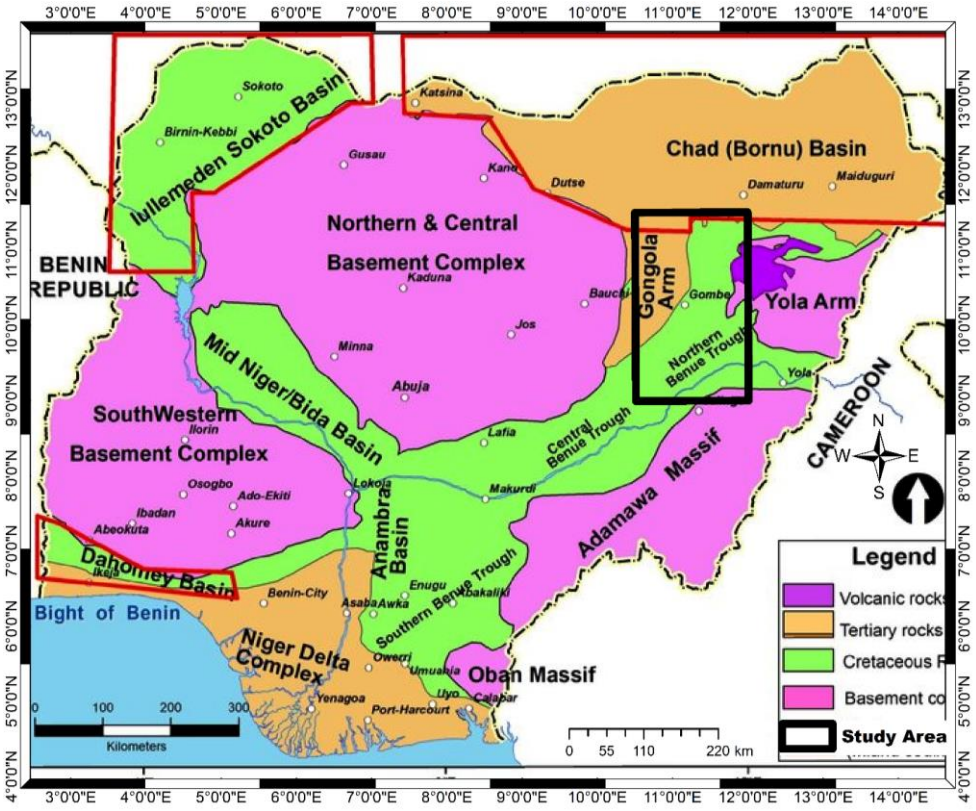

Figure 1.1: Location map of study area

ISSN No. 2454-6194 | DOI: 10.51584/IJRIAS |Volume IX Issue IX September 2024

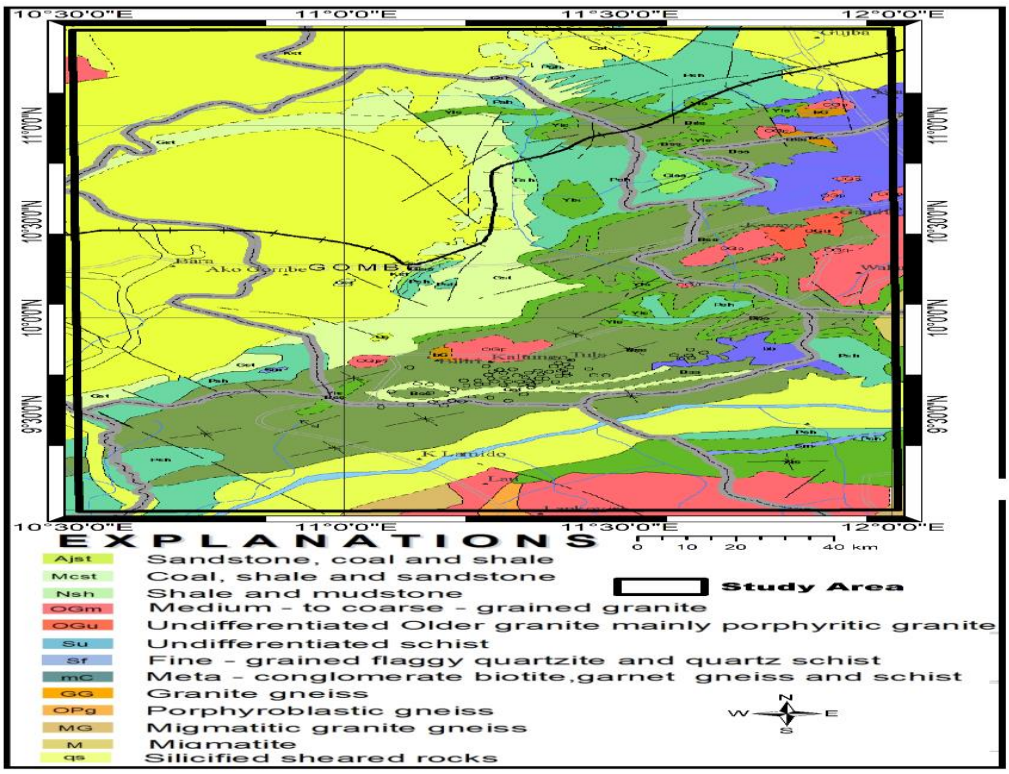

Figure 1.2: Geology map of study area

Pseudogravimetric Transformation

The pseudogravity computation is based on Poisson's relation which shows that the magnetic potential (V) and the gravitational potential (U) for a body with the ratio of density to magnetization constant at each point, and the magnetization vector in a constant direction are related by directional derivatives in three-dimensions;

$$\boldsymbol{V_{x,y,z} = \frac{C_m M}{G\rho}\frac{\partial U_{x,y,z}}{\partial m}, \frac{M}{\rho} = constant} \qquad (1.1)$$

Where ρ is the density contrast, M is the intensity of magnetization contrast, m is a unit vector in the direction of total magnetization and G is the gravitational constant.

The magnetic field anomaly $T_{x,y,z}$ at an external point due to a body is related to the magnetic potential (V) as (Tandrigoda & Ofoegbu (1989);

$$\boldsymbol{T_{x,y,z} = \frac{\partial V_{x,y,z}}{\partial f}} \qquad (1.2)$$

Where f represents a unit vector in the direction of Earth's total field. Substituting equation 1.1 into equation 1.2, we obtain:

$$T_{x,y,z} = \frac{C_m M}{G\rho}\frac{\partial U_{x,y,z}}{\partial f \partial m} \qquad (1.3)$$

It is possible therefore to compute a theoretical gravity potential U from any given measured magnetic anomaly T (x, y, z) and from this gravitational potential, a pseudogravity anomaly ∇U can be computed. This pseudogravity anomaly is not the true gravity anomaly due to the body, but a fictitious anomaly completely derived from a true magnetic anomaly assuming the ratio ($\frac{M}{\rho}$) to be constant throughout the source body. From equation 1.3, the pseudogravimetric potential is obtained:

$$\boldsymbol{U = \frac{G\rho}{C_m M}\int_{-\infty}^{\infty}\int_{-\infty}^{\infty} T_{x,y,z}\, \partial f \partial m} \qquad (1.4)$$

ISSN No. 2454-6194 | DOI: 10.51584/IJRIAS |Volume IX Issue IX September 2024

Taking the fictitious density contrast to be equal to:

$$\rho = \frac{C_m M}{G}$$

The pseudogravimetric anomaly is then given by:

$$g_{x,y,z} = \frac{dU}{dz} = \frac{d}{dz}\int\int_{-\infty}^{\infty} T_{x,y,z}\, df\, dm \qquad (1.5)$$

Taking Fourier transform of both sides, we obtained:

$$\boldsymbol{F(g_{x,y,z}) = F(H_f) * F(T_{x,y,z})} \qquad (1.6)$$

H_f = Filter that transforms the total-field anomaly $\boldsymbol{T_{x,y,z}}$ measured on the horizontal surface into the Pseudogravity anomaly $\boldsymbol{g_{x,y,z}}$.

The Fourier transform of the pseudogravity transform filter is given by (Blakely, 1995):

$$F(H_f) = \frac{k}{(|k|f_z + ik_x f_x + ik_y f_y)(|k|m_z + ik_x m_x + ik_y m_y)} \qquad (1.7)$$

k_x,k_y are wavenumbers in the direction of x and y axis respectively, $(m = m_x, m_y, m_z)$ and $f = f_x + f_y + f_z$re unit vectors of ambient magnetic field and magnetization field with respect to x, y, z axis.

The process consists of three steps; Fourier transformed the magnetic field anomaly $F(|T|_{x,y,z}$, multiplied by the filter $F(|H|_f$ and then inversed Fourier transformed the product. The process requires a 2D gridded magnetic field map.

Pseudogravity transform can also be carried out by the vertical integration of the reduced to pole anomaly (Blakely, 1995).

RESEARCH METHODOLOGY

Materials

The materials needed for this study are;

The data used for the research were TMI sheets: 108 (Akwiam), 109 (Nafada), 110 (Mutwe), 130 (Duku), 131 (Bajoga), 132 (Gulani), 151(Ako), 152 (Gombe), 153 (Wuyo), 172 (Futuk), 173 (Kaltungo), 174 (Guyok) obtained from the Nigerian Geological Survey Agency (NGSA). The aeromagnetic survey had a flight line spacing of 500m, sensor mean terrain clearance of 80m, and tie line spacing of 5000m.

Satellite Gravity data of the study area obtained from International Center for Global Earth Models (ICGEM).

Oasis Montaj Software version 8.4 has been used for processing and the data and estimating source parameters.

Pseudogravimetric transformation of the gridded data

The interpretation of magnetic anomalies is complicated due to the inclined magnetization of their sources and the inclination of the ambient field. The shape of a magnetic anomaly relative to its source is distorted by these parameters causing a decrease in the amplitude of the anomaly, asymmetry in the anomaly and shift of the peak of the anomaly to the south in the northern geomagnetic hemisphere and the converse in the southern geomagnetic hemisphere. Baranov (1957) introduced the concept of pseudogravimetric transformation to correct the distortions. The pseudogravimetric transformation converts magnetic field data into gravity-like data generally called pseudogravimetric data. The transformation, among other things removes the asymmetrical

ISSN No. 2454-6194 | DOI: 10.51584/IJRIAS |Volume IX Issue IX September 2024

nature of the magnetic anomaly, enhances the regional anomalies that are due to deeper sources, attenuate the anomalies that are due to shallow sources and generally highlights the density variations in the area. The Pseudogravimetric filter in the Fourier domain is given by: -

$$(H_f) = \frac{k}{(|k|f_z + ik_x f_x + ik_y f_y)(|k|m_z + ik_x m_x + ik_y m_y)} \qquad (1.8)$$

The Total Horizontal Derivative of the Pseudogravimetric Anomaly

The magnitude of the total horizontal gradient of the pseudogravity anomaly is given by:

$$HDR = \sqrt{\left(\frac{\partial T}{\partial x}\right)^2 + \left(\frac{\partial T}{\partial y}\right)^2} \qquad (1.9)$$

The horizontal gradient can be applied to a 2D grid of gravity or Pseudogravimetric Anomaly, and through visual inspection, the steepest gradients can be located highlighting the locations of major density or susceptibility contrasts. This can include faults, the edges of bodies, or lateral compositional changes.

The Tilt Angle of the Pseudogravimetric Anomaly

The tilt angle normalizes the vertical derivative by the total horizontal derivative so that the vertical derivative will not vary with size of anomaly. It is the arctangent of the vertical derivative to the total horizontal derivative (Salem et al., 2008).

$$TiltAngle(\theta) = tan^{-2}\left[\frac{\frac{\partial T}{\partial z}}{\sqrt{\left(\frac{\partial T}{\partial x}\right)^2 + \left(\frac{\partial T}{\partial y}\right)^2}}\right] = \frac{FVDR}{THDV} \qquad (1.10)$$

The tilt angle yields a result that gives equal emphasis to both large and smaller anomalies. The tilt angle ranges from -90 to + 90 degrees, is positive over the magnetic source, and negative outside the source with the edges of the sources delimited by the 0-degree contour. It is useful in highlighting subtle features in magnetic data (Foss, 1989).

Spectral Analysis

The spectral depth method is based on the principle that a magnetic field measured at the surface can be considered to represent a series of components of different wavelengths of different sizes and directions from all depths. The logarithmic of the power of the signal at each wavelength can be plotted against wavelength, regardless of direction to produce a power spectrum. The power spectrum is observed to be broken up into a series of straight-line segments. Each line segment represents the cumulative response of a discrete ensemble of sources at a given depth. The depth is directly proportional to the slope of the line segment.

The application of the power spectrum method to potential field data was proposed by Bhattacharyya (1966); and the determination of the average depths of source ensembles was given by Spector and Grant (1970). This method has been used extensively by many researchers like Salako and Udensi (2013); Ofoegbu and Hein (1991). This technique can be used to identify the characteristic depth of the magnetic basement on a moving window by selecting the steepest straight-line segment of the power spectrum. A depth solution is calculated for the power spectrum derived from each grid subset. In its complex form, the two-dimensional Fourier transform pair may be written as in equations 1.11 and 1.12 (Bracewell, 2000):

$$G(u,v) = \iint_{-\infty}^{\infty} g(x,y)e^{i(ux-vy)}dxdy \qquad (1.11)$$

$$g(x,y) = \frac{1}{4\pi^2}\iint_{\infty}^{\infty} G(u,v)e^{-i(ux-vy)}dudv \qquad (1.12)$$

ISSN No. 2454-6194 | DOI: 10.51584/IJRIAS |Volume IX Issue IX September 2024

g (x, y) represents the signal in space domain, G (u, v) represents the signal in wavenumber domain, u and v are the angular frequencies in x and y directions respectively. G (u, v) is generally complex and can be expressed into its real and imaginary parts given as:

$$G(u,v) = P(u,v) + iQ(u,v) \quad (1.13)$$

It can also be written as:

$$G(u,v) = |G(u,v)|e^{i\theta(u,v)} \quad (1.14)$$

where,

$$|G(u,v)| = \left[\left(ReG(u,v)\right)^2 + \left(ImG(u,v)\right)^2\right]^{\frac{1}{2}} \quad (1.15)$$

$$\theta(u,v) = arctan\left[\frac{ImG(u,v)}{ReG(u,v)}\right] \quad (1.16)$$

|G (u, v) | and $\theta(u,v)$ are called the amplitude spectrum and the phase spectrum respectively. The power spectrum |G (u, v) |^{2}and its total energy spectrum is given by:

$$|G(u,v)|^2 = Re|G(u,v)|^2 + Im|G(u,v)|^2 \quad (1.17)$$

$$E_T = \frac{1}{4\pi^2}\iint_{\infty}^{\infty}|G(u,v)|^2 dudv \quad (1.18)$$

Estimation of depth to the top of magnetic sources follows from the power spectrum (PS) due to an ensemble of magnetic sources that are at an average depth z from the observation elevation:

$$PS(k) = Ce^{-4\pi zf} = Ce^{-2zk} \quad (1.19)$$

The exp (-2zk) term is the dominant factor in the power spectrum. $k = 2\pi f = 2\pi/\lambda$ in radians/unit distance. C is a constant which includes field parameters and magnetic properties.

Taking the natural logarithm of both sides of equation 1.22, yields the linear equation:

$$\ln[PS(k)] = ln[C] - 4\pi zf = ln[C] - 2zk \quad (1.20)$$

Where ln[C] is the intercept and $4\pi z$ or 2z is the slope of the straight-line plot of ln [PS] vs f or k respectively.

$$slope = -2z$$

The mean depth (z) to a statistical ensemble of sources can be determined by the following expressions:

$$z = -\frac{Slope}{2} \quad (1.21)$$

The power spectrum generally has two sources. The deeper source is manifested in the smaller wavenumber end of the spectrum, while the shallower ensemble manifests itself in the larger wavenumber.

Digital signal processing software (OASIS MONTAJ), employing the fast Fourier transform technique was used to transform the total magnetic data into the radial energy spectrum for each block. For easier handling of the large data involved, the study area was divided into 35 spectral cells (labeled 1- 35) in table below of 10 km by 10 km to accommodate longer wavelength so that depth up to about 10 km could be investigated.

Graphs of logarithm of the power spectrum against frequencies for the 35 spectral cells were plotted as shown in Figure 1.4. For each cell, two linear segments could be identified which implies that there are two magnetic source layers in the study area. Each linear segment group points are due to anomalies caused by bodies occurring

ISSN No. 2454-6194 | DOI: 10.51584/IJRIAS |Volume IX Issue IX September 2024

within a particular depth range. The line segment in the higher frequency range is from the shallow sources and the lower harmonics are indicative of sources from deep - seated bodies.

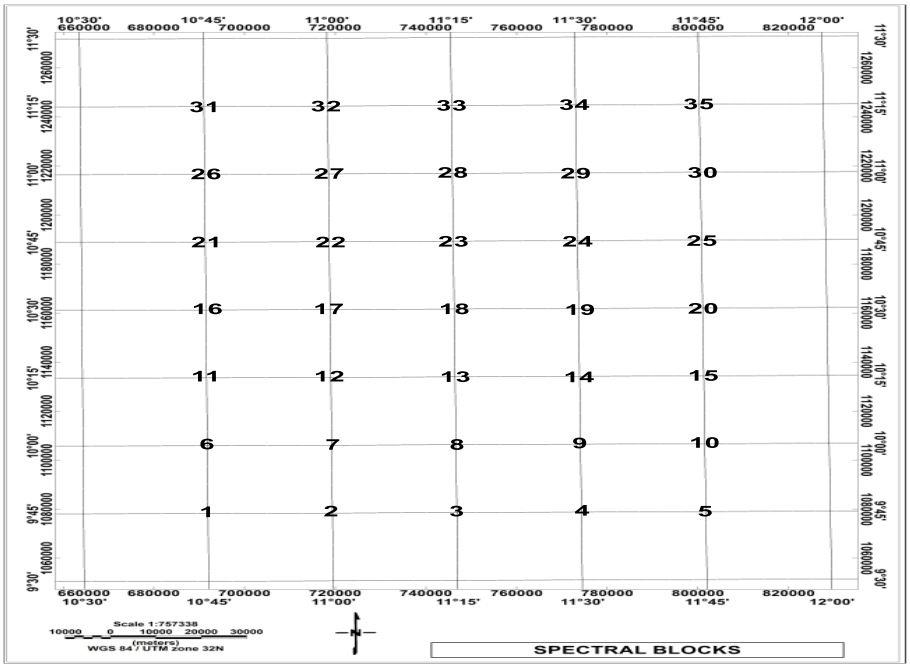

Figure 1.3: Spectral cell blocks for spectral analysis.

Block 1

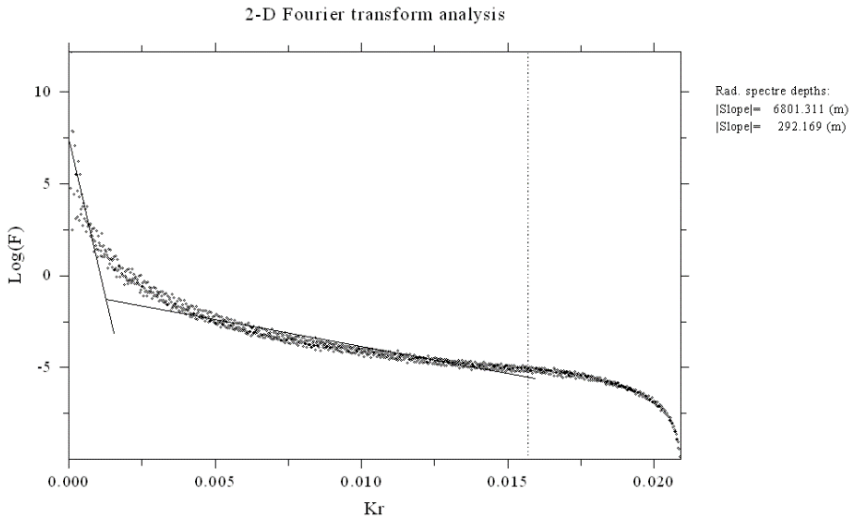

Figure 1.4:

RESULTS

Gridded Total Magnetic Intensity (TMI) Map of Study area.

Figure 1.5 is the total magnetic field intensity (TMI) of the study area. It reveals the magnetic response that is due to the various lithological units in the study area. The minimum value of the magnetic intensity in study is -172.9 nT and the maximum value is 195.1. The magnetic anomalies observed reflect the magnetic susceptibility contrast between the magnetic crystalline basement and the Cretaceous to Tertiary age sediments. Unfortunately, in the study area, the inclination of the Earth's magnetic field vector is low and the total magnetic intensity map is, therefore, difficult to interpret for location and strike of magnetic bodies. therefore, the gridded TMI map of the study area as shown in figure 1.5 have the amplitude of their magnetic anomalies attenuated and skewed from their perturbing sources. The problem is more complicated if the anomalies are close to the equator because

ISSN No. 2454-6194 | DOI: 10.51584/IJRIAS |Volume IX Issue IX September 2024

ambient field is horizontal and structure striking N-S are attenuated. Transformations such as reduction to the pole (RTP), Analytic Signal (AnaSig) and Pseudogravimetric (PSG) transformation (PSG) have become standard in the processing and interpretation of magnetic anomalies because among other advantages, they can restore the anomalies back to over their perturbing sources.

Pseudogravimetric transformation of the Total Magnetic Field Intensity (TMI)

Figure 1.6 is the Pseudogravimetric Anomaly transformed of the Total Magnetic Field Intensity of Figure 1.5. The Pseudogravimetric transformation filter is a low- pass filter, and has some noticeable effects on the Total field intensity map (Figure 1.5) which includes filtering out the short wavelengths anomalies that are due to shallow features and enhancing the low frequency anomalies that are due to deeper sources. Therefore, the resultant effect of the transformation will be of broad-based regional anomalies that are due to deeper magnetic structures. The maximum value of the pseudogravimetric anomaly is 19.7 milliGal, the minimum is -42.4 milliGal. Two broad, positive, regional Pseudogravimetric anomalies can be identified in Figure 1.6 which are due to formations with high pseudo-density values flanking a sub-basin. Overall, the structure shown in the pseudogravimetric map is a result of the low-pass filter effect on the TMI giving rise to regional structures that is probably a graben/horst fault. The central depression filled sediments can be interpreted as a graben filled with Cretaceous sediments. The existence of block faulting has been suggested in the area by Shemang et al. (2004). Also, the positive magnetic anomalies that occupy the central region in figure 1.5 have been replaced with negative magnetic anomalies (Figure 1.6), indicating a 90^{o} phase shift from the magnetic equator to the pole. The phase shift to the pole and the attenuation of the high frequency components of the anomalies is the composite result of the pseudogravimetric transformation procedure, which mathematically consist of two procedures: the vertical integration of the reduced to pole transformations.

Satellite gravity of the study area

The Satellite gravity anomaly map (Figure 1.7) of the study area vary from a low of -43.2 mGal to a high of -29.5 mGal. They are generally low in the northern part and high in the southern part. The Satellite gravity map shows a regional variation from SW (high values) to NE (low values). The low gravity values in the northern part may be attributable to a thick lower density sedimentary basin, while the high value in the southern part may be attributable to an igneous intrusions or uplifted basement rocks. Gravity gradient seen in the middle of the study area indicate the presence of a major fault system.

Comparison between the pseudogravimetric anomaly map and the satellite gravity map

Comparing the satellite gravity field Intensity Map (Figure 1.7) and the Pseudogravimetric transformed (PSG) anomaly Map (Figure 1.6), we will immediately notice as shown in Figure 1.8 that there is a positive correlation between them in the southern part and negative correlation in the northern part of the study area. As can be seen they are in phase in the southern part and out of phase in the northern part of the study area. This suggests that there is a common source of both the gravity anomaly and the magnetic anomaly. In the northern part where they do not coincide is an intra-sedimentary magnetic anomaly (i.e. a sedimentary section with high magnetic susceptibility), is indicative of possibly a thick sedimentary basin with magnetic minerals. There is also a correlation in density variation between the satellite gravity map (figure 1.7) and the geological map (Figure 1.2). Anomalous magnetization may arise in sedimentary basin because of processes such as Detrital remanence magnetization (DRM) or Diagenetic magnetite or pyrrhotite formed by hydrocarbon plumes.

The Total Horizontal Derivative of the Pseudogravimetric Anomaly

The total Horizontal Derivative usually shows maxima over regions of discontinuity within the pseudogravimetric data (e.g. lithology boundaries, faults or dykes). In this context, therefore, the figure (1.9) shows several peak values of the total horizontal derivative over some areas in the Study area. Some are lithology boundaries between basins and basement highs while some are faults. Some are trending W-E, while some are trending SW-NE. Some of the trending SW-NE are around Gombe fault and Kaltungo fault and the Burashika fault. Among those edges are boundaries between horst and graben structures which are evidence of crustal extension and the subsequent block faulting.

ISSN No. 2454-6194 | DOI: 10.51584/IJRIAS |Volume IX Issue IX September 2024

Tilt Angle of the Pseudogravimetric Anomaly

The Tilt angle mathematically normalizes the vertical derivative and highlights potential field anomalies irrespective of their size and depth. This makes the Tilt angle function like an Automatic Gain Control (AGC) Filter. From the figure (1.10), the area is structurally marked by numerous SW-NE linear intrusive igneous features of positive tilt angles that are bounded by negative or zero tilt angles values. The tilt angles are positive over a source with high pseudo-density values, negative over sources with low pseudo-density values and zero over vertical contacts. There are numerous alternating positive and negative values of pseudogravimetric values. These are contacts between sedimentary rock units and igneous rock units or between a horst and graben. In the middle of the study trending west-east are negative values of the tilt angle indicating that they are sedimentary sub-basins or graben depressions.

Lineament of the study area

Underlying structures such as faults and fractures often manifest themselves on the Earth surface as linear features. These linear features are called Lineaments. Lineaments helps in understanding the underlying stress regions and tectonic processes. They also act like guides in exploring for minerals and hydrocarbon. Figure 1.11 is the lineament map of the study area. Most of lineaments are: NE-SW, E-W, NW-SE. The predominant and longer lineaments are those trending NE-SW and the E-W while a few attending NW-SE. As can be seen in Figure 1.11, the lineaments vary in length and density. Areas with high density of lineaments often correlate with fractures and areas of mineralization. The longer lineaments correlate with faults.

Results of Spectral Analysis.

Table 1 shows an estimate of the depth values of the magnetic sources from shallow sources (Z_2) and deeper sources (Z_1). For the shallow sources, the minimum depth is 160.8 m, the maximum depth is 534.8 m, while the average minimum depth is 296.4 m. For the deep magnetic sources, the minimum depth is 4.20 km, the maximum depth is 10.4 km, while the average maximum depth is 7.75 km. The magnetic sources that account for the shallow sources are the intra-sedimentary magnetic rock units that intrude the Cretaceous sedimentary basin. They are of short wavelengths and discrete. The magnetic sources that are accountable for the deeper sources are the result of irregular topography of the magnetic basement. They impact regionally on the study area because of their large wavelengths. The magnetic sources of the deeper basement may include fault planes and intra-basement magnetic bodies.

The depth to the deeper magnetic basement as determined by the spectral analysis method agrees well with the Source parameter method as determined above. It also agrees well with the interpretation of the aeromagnetic data over the trough by Ofoegbu (1988). It also agrees with those of Nur (2001); Nur et al. (2003) and Salako (2014). Making use of Z_1 (Deeper sources) and Z_2 (Shallow sources) data of table1, the magnetic basement surface contour plots of Z_1 and Z_2 (Figures 1.12 & 1.14) and their corresponding 3-D Model plots (Figures 1.13 & 1.15) are plotted with Surfer32.

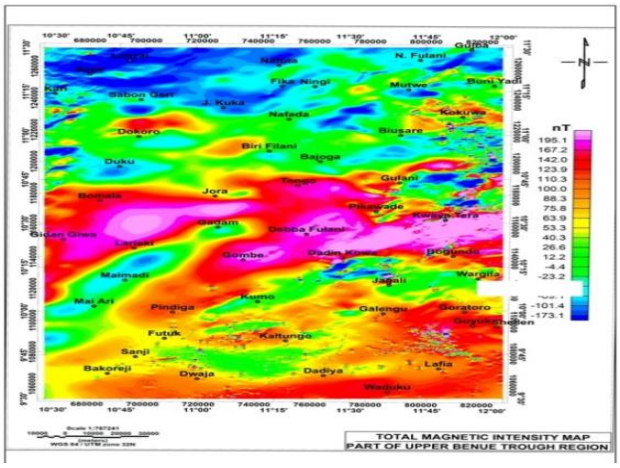

Figure 1.5: Total Magnetic field Intensity Map (TMI) of the study area

ISSN No. 2454-6194 | DOI: 10.51584/IJRIAS |Volume IX Issue IX September 2024

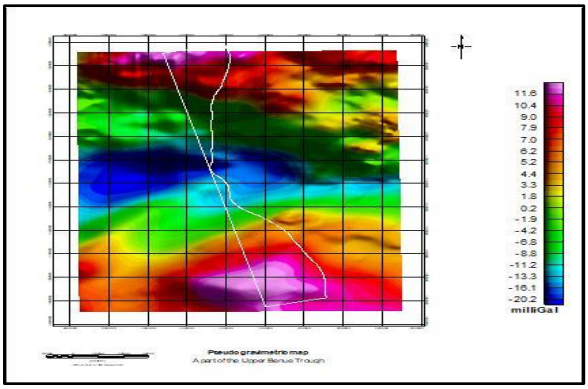

Figure 1.6: Pseudogravimetric (PSG)Anomaly Map transformed from the Total Magnetic Intensity (TMI) Map Figure (4.1) with a profile

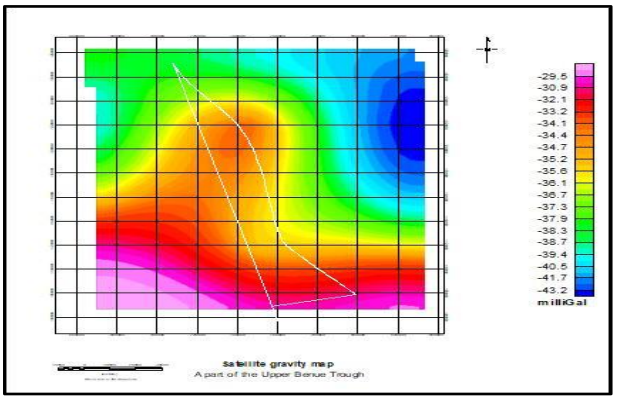

Figure 1.7: Satellite gravity map of study area.

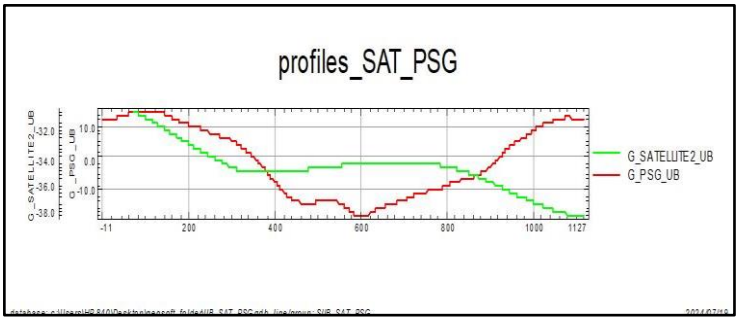

Figure 1.8: Comparison of the same profile across PSG map (red) and satellite gravity map (green). The profiles are in phase in the southern part of the study area indicating a common source while they are out of phase in the northern part.

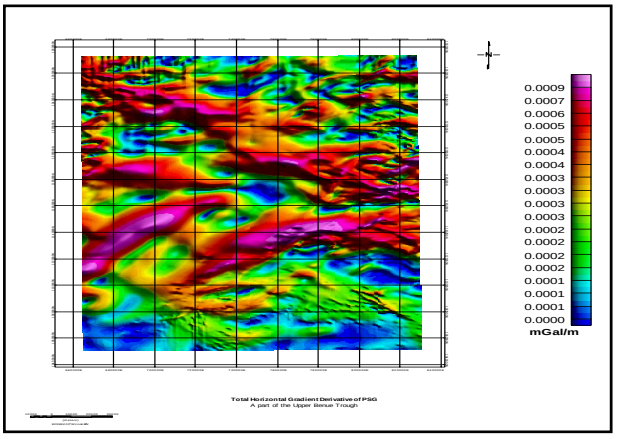

Figure 1.9: The total Horizontal Derivative (THD) of the Pseudogravimetric (PSG) Anomaly

ISSN No. 2454-6194 | DOI: 10.51584/IJRIAS |Volume IX Issue IX September 2024

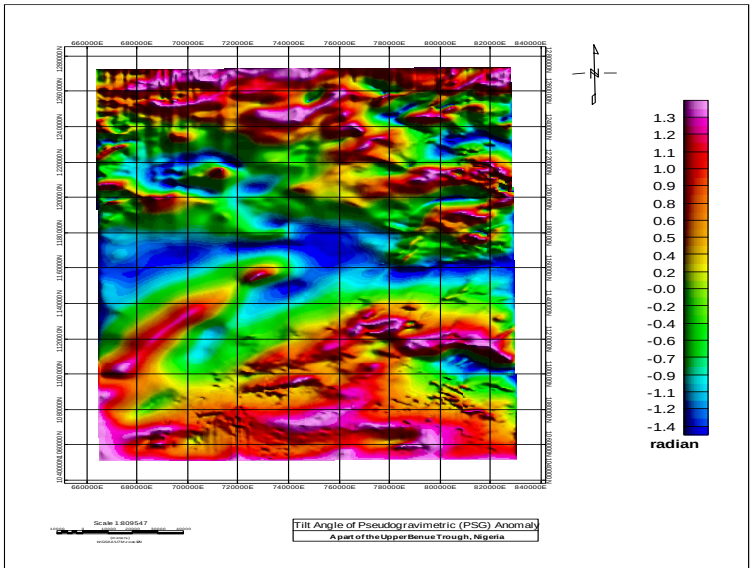

Figure 1.10: Tilt angle of the Pseudogravimetric (PSG) anomaly

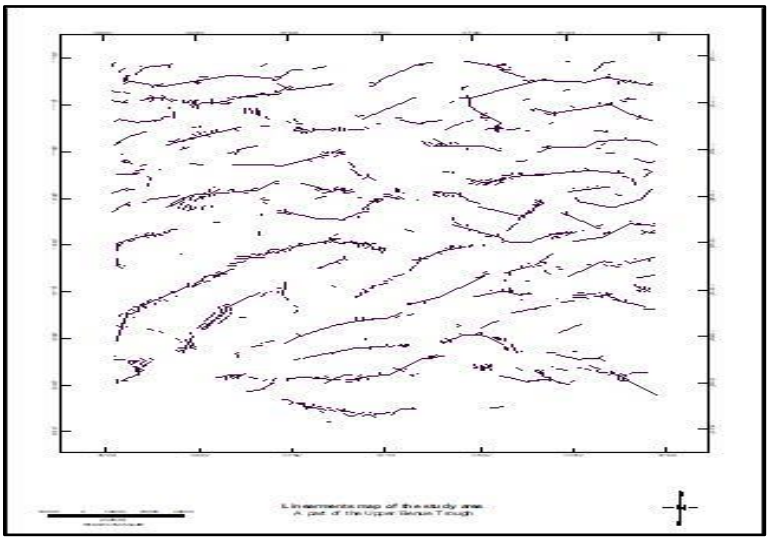

Figure 1.11: Lineament map of the study area obtained from the PSG anomaly.

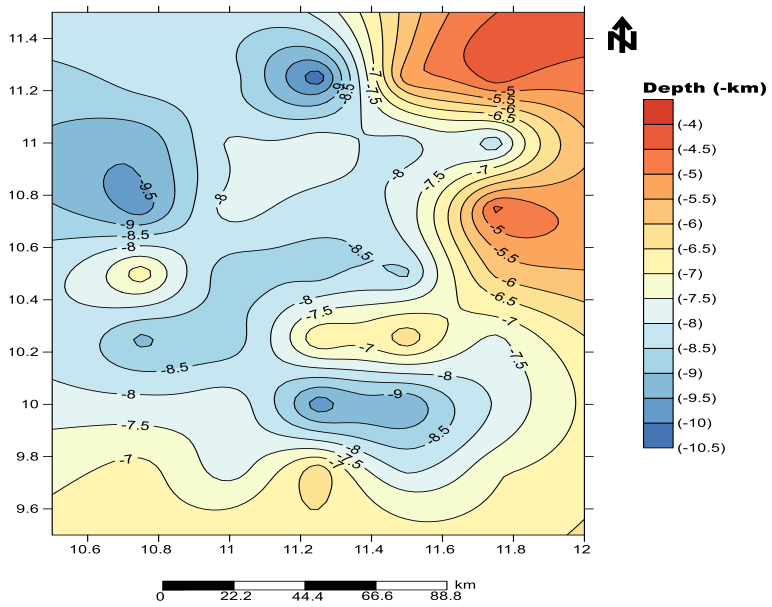

Figure 1.12: 2-D Contour Plot of the deep Magnetic Basement Surface Z_1, Contour interval 0.05.

ISSN No. 2454-6194 | DOI: 10.51584/IJRIAS |Volume IX Issue IX September 2024

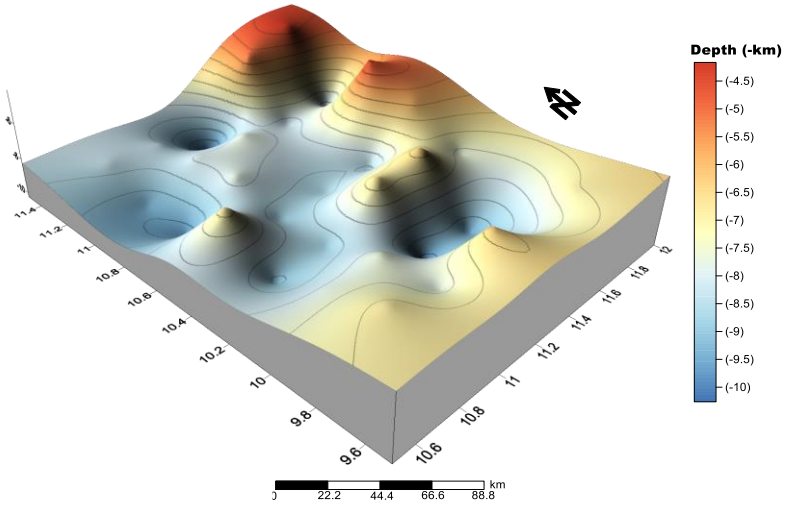

Figure 1.13: 3-D Model of the Deep Magnetic Basement Surface (Z_1) of the study area

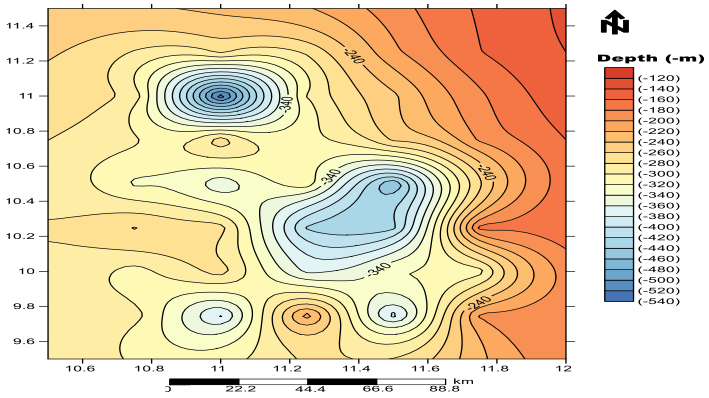

Figure 1.14: 2-D Contour Plot of the shallow Magnetic Basement Surface Z_2.

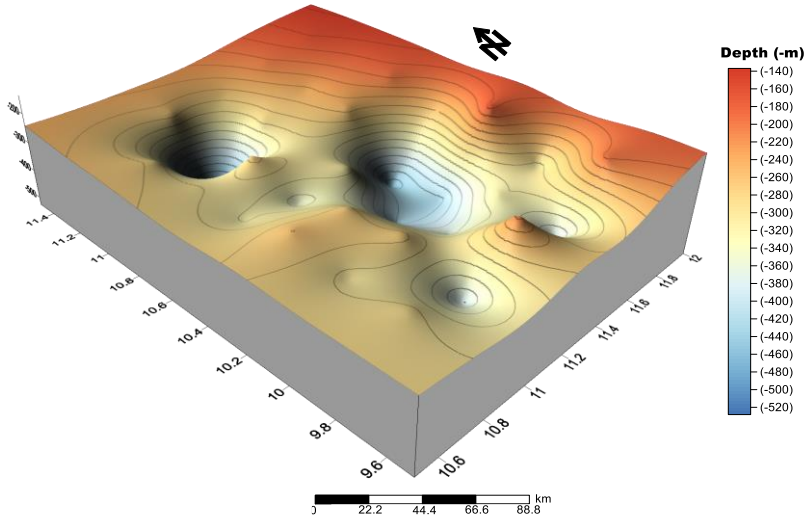

Figure 1.15: 3-D Model of the shallow Magnetic Basement Surface (Z_2) of the study area.

DISCUSSIONS

Summary

A Pseudogravimetric study of a part of the Upper Benue Trough, Nigeria has been carried out. The total field Intensity (TMI) has been transformed into a gravity anomaly called the Pseudogravimetric Anomaly. The overall effect of the transformation has been to reduce the field intensity to pole, attenuate the high frequency anomalies that are due to shallow sources and to enhance the low frequency anomalies that are due to deeper sources.

The Enhancement of the Pseudogravimetric (PSG) by various derivatives; first vertical derivative, analytical signal, total horizontal derivative, and the tilt angle has revealed the magnetic anomalies to be due to a combination of igneous intra-sedimentary intrusions, intra-basement magnetic bodies, fault lineaments, horst/graben structure and diagenetic (chemical remanent) magnetic sources. Negative Pseudogravimetric anomalies are associated with low density sedimentary basins. The crystalline basement depth has been determined using the Source Parameter Imaging. The minimum and the maximum depth as modelled by the (SPI^{TM}) method are 443 m and 7.51 km. The ranges also agree well with that of other scholars.

CONCLUSIONS

The use of pseudogravimetric transformation has proven to be a good tool for studying the evolution and history of the Upper Benue trough. The analysis of the pseudogravimetric anomaly by comparing it with the satellite gravity data and using the derivatives of the pseudogravimetric data such as horizontal derivative and the tilt angle has provided valuable insights into the geological structure of the magnetic bodies underneath the study area. Comparing the pseudogravimetric anomaly map and the satellite gravity map has revealed a common source of the anomalies in the southern part of the study area. Also, the findings of the study include the identification of igneous intrusions, intra-basement sources, topography of the basement and variable magnetic susceptibility has contributed to the understanding of the regions geological processes and evolution. The evolution of the Benue trough is thought to have involved tensional forces that led to the stretching and thinning of the Earth's crust resulting in the formation of the rift system. The tensional forces are believed to be driven by the mantle plume activity. The mantle plume theory suggests that hot, buoyant upwellings of magma from the Earth's mantle can create stretching and thinning of the Earth's crust, resulting in the formation of the rift system. Continued stretching and thinning is believed to have been accompanied by more pronounced zones of weakness and possibly subsidence. Continuous mantle plume activity and updoming gave rise to the emplacement of intrusive bodies along the lines of weakness and consequently block faulting. The continued emplacement of intrusive materials enhanced the breakup of the crust and block faulting, giving rise to the formation of graben (down-dropped blocks) and horst (uplifted blocks) structural features which gives the magnetic basement a rather irregular topography. Future research including integrating additional geophysical methods, detailed petrological and geochemical analysis of rock samples and Long-term monitoring of the magnetic field variations through time-lapse analysis can assist in understanding the geological structure and resource potential of the area.

AKNOWLEDGEMENTS

I would like to extend my appreciation to Tertiary Education Trust fund (TEDFund) for providing the funding for the data and software used in this research. Many thanks to the staff of the department of physics, Nasarawa state university for their support and professional guidance.

REFERENCES

1. Ahmed, s., Chris, O., Samuel, C., Derek, F., & Essan, A. (2013). Mapping the depth to magnetic basement using inversion of pseudogravity; application to the bishop model and the stored basin, northern North Sea. Geophysics, 2(2). 69-78. http://DOI:10.1190/INT-2013-0105.1.
2. Baranov, V. (1957). A new method for interpretation of aeromagnetic maps pseudo-gravimetric anomalies; Geophysics. (22), 359-383.
3. Blakely, R.J. (1995). Potential Theory in Gravity and Magnetic Applications. Cambridge University Press.
4. Bracewell, R. N. (2000). The Fourier Transform and its Applications (3rd edn). McGraw-Hill Book Co.
5. Crachley, C. R., & Jones, J. P. (1965). An interpretation of the geology and gravity anomalies of the Benue valley, Nigeria. Overseas geological Survey, Vol. 9, 1-28.
6. David, A. P. and Zhiqum, S. (2004). An improved pseudogravity magnetic transform technique for investigation of deep magnetic source rocks, ASEC Extended Abstracts, 2004:1, 1-4. http://DOI.10.1071/ASEC2004ab116.
7. Foss, C. 1989. Magnetic data Enhancement and Depth Estimation. In the Encyclopedia of Solid Earth

Geophysics. Gupta, H.K., ed. Springer, Netherlands. Pp736-746.
8. Henderson, R., Miyazaki, Y., & Wold, R. (1984). Direct indication of hydrocarbons from airborne magnetic. Exploration Geophysics, 15, 213-219.
9. Hinze, W.J., Von Frese, R.R.B., Saad, A.H. (2012). Gravity and Magnetic Exploration; Principles, Practices and Applications. Cambridge University Press.
10. Getech. (2008). Advance processing and Interpretation of gravity and magnetic data. Getech.
11. Nur, A. (2001). Analysis of aeromagnetic data over the Yola arm of the Upper Benue Trough, Nigeria. Journal of Mining and Geology, 36, 77-84.
12. Nur, A., Ofoegbu, C. O., Onuoha, K. M. (2003). Spectral analysis and Hilbert Transform of aeromagnetic data over the Upper Benue Trough, Nigeria. Global Journal of Geological Sciences, 1(2), 129- 142.
13. Obaje, N.H. (2009). Geology and Mineral Resources of Nigeria. Springer.
14. Ofoegbu, C.O (1985). A review of the Geology of the Benue Trough, Nigeria. Journal of African Earth Sciences, 3(3) 283-291.
15. Ofoegbu, C.O. (1985). Preliminary result from a pseudogravity study of the Benue-Trough Nigeria. Journal of African Earth Sciences, (5) 187-192.
16. Ofoegbu, C, O. (1988). An aeromagnetic study of part of the Upper Benue Trough, Nigeria. Journal of African Earth Science, 7(1) 77-90.
17. Ofoegbu, C, O. (1984). Interpretation of aeromagnetic anomalies over the lower and middle Benue Trough of Nigeria. Geophysics, 79(3), 813-823.
18. Ofoegbu, C, O., & Hein, K. (1991). Analysis of Magnetic Data over part of the younger granite province of Nigeria. PAGEOPH, 136(23).
19. Panepinto, S., luca, L.D., Mantovani, M., & Sfolciaghi, M. (2014) Using Pseudogravity functional transform to enhance deep magnetic sources and enrich regional gravity data. [Conference presentation]. Denver, 1275-1279
20. Pratt, D.A. & Zhiqun, S. (2004). An improved pseudo-gravity magnetic transform technique for investigation of deep magnetic source rocks. [Conference presentation] ASEG 17th Geophysical Exploration and Exhibition, 1-4, DOI; 10.1071/ASEG2004ab116.
21. Reeves, C. (2005). Aeromagnetic Surveys: Principles, Practice and Interpretation. Geosoft E-book. http://www.geosoft.com/media/uploads/resources/technicalpapers/Aeromagnetic.
22. Salako, A. K. (2014). Depth to basement determination using Source Parameter Imaging (SPI) of aeromagnetic data: an application to Upper Benue Trough and Borno Basin., Northeast, Nigeria. Academic Research International, 5(3).
23. Salem, A., Williams, S., Fairhead, D., Smith, R. Ravat, D. (2008). Interpretation of Magnetic data using Tilt Angle Derivative. Geophysics, 73(1) 1-10.
24. Shemang, E.M., Jacoby, W.R., Ajayi, C.O. (2004). Gravity Anomalies over the Gongola arm, Upper Benue Trough, Nigeria. Global Journal of Geological Sciences 3(1). 61-69.
25. Spector, A. and Grant, F. S. (1970). Statistical Models for Interpreting Aeromagnetic data. Geophysics, 35(2), 293-302.
26. Tandrigoda, D.A, &Ofoegbu, C.O (1989). A Routine for the Rapid Computation of the Pseudogravity field. Inverse modelling in Exploration Geophysics. Friedr, Vieweg and Sohn, Wiesbaden, 93-109.
27. Verduzco, B., Fairhead, J.D., Green, C.M., and Mackenzie, C. (2004). New insights into magnetic derivatives for structural mapping: The Leading Edge, v. 23, p. 116- 119
28. Wright, J. B. (1968). South Atlantic Continental Drift and the Benue Trough, Tectonophysics, 6(4), 301-310, https://doi.org/10.1016/0040-1951(68)90046-2
29. Zhou, W. (2018). Aeromagnetic Survey. In Encyclopedia of Engineering geology. Encyclopedia of Earth Sciences Series. Bobrowsky, P.T., Marker, B. (Ed). Springer, Cham. https:// doi.org/ 10.1007/ 978-3 -319 -73556898.

ISSN No. 2454-6194 | DOI: 10.51584/IJRIAS |Volume IX Issue IX September 2024

APPENDIX

Spectral Blocks

Blocks 1 & 2

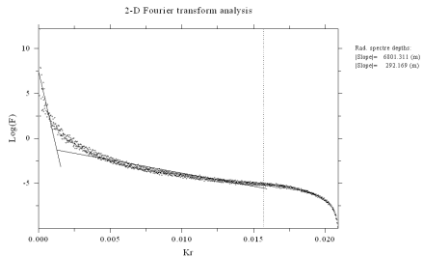

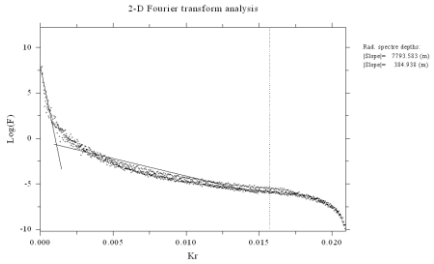

Blocks 3 & 4

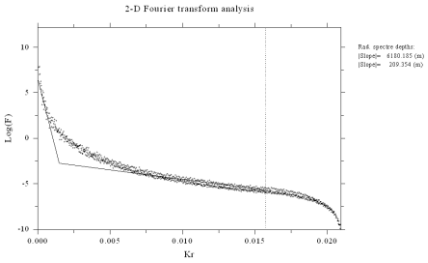

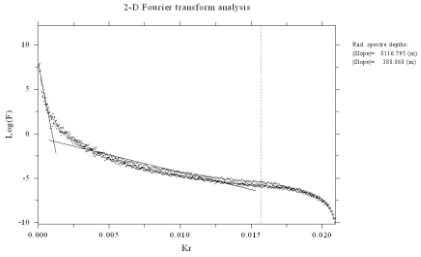

Blocks 5& 6

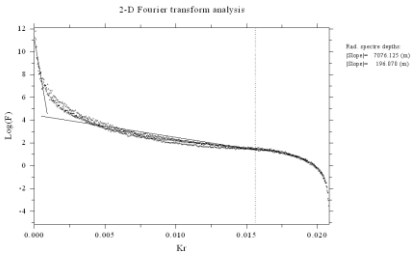

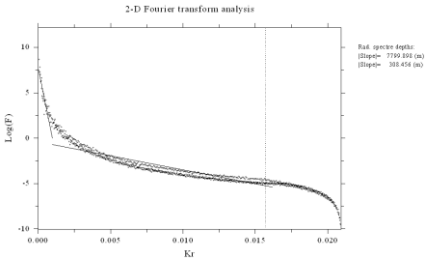

Blocks 7 & 8

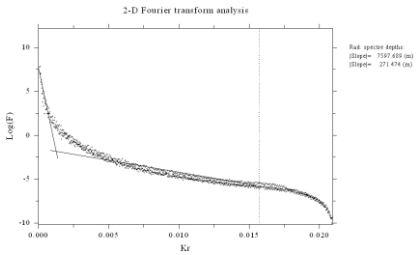

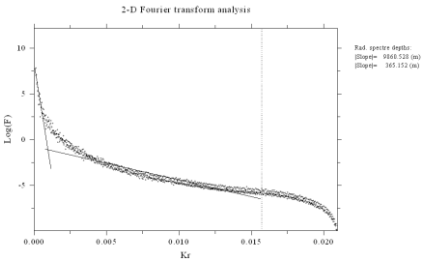

Blocks 9 & 10

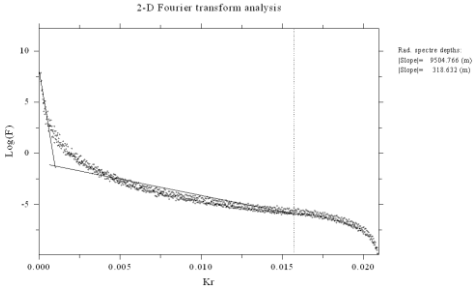

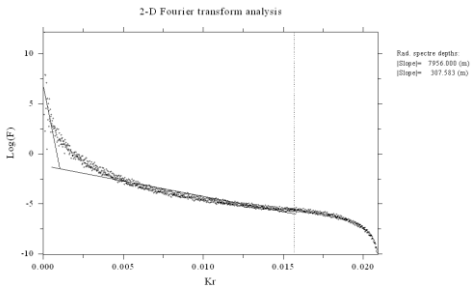

ISSN No. 2454-6194 | DOI: 10.51584/IJRIAS |Volume IX Issue IX September 2024

Blocks 11 & 12

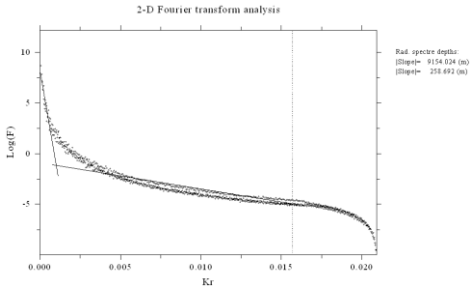

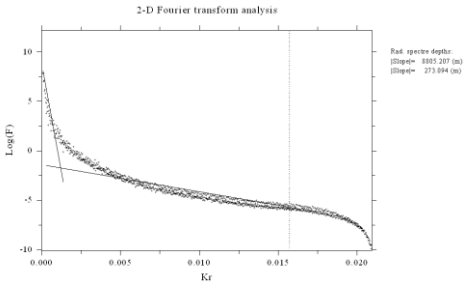

Blocks 13 & 14

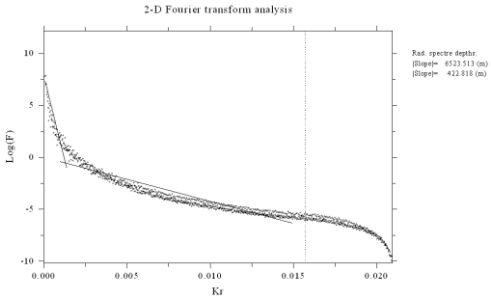

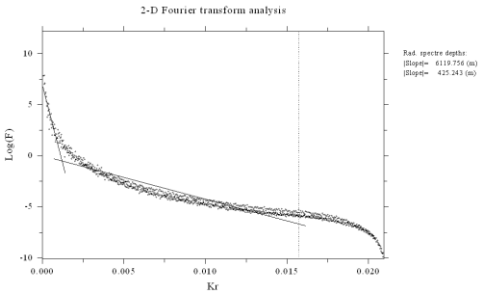

Blocks 15 & 16

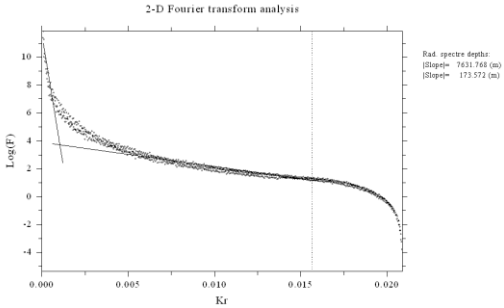

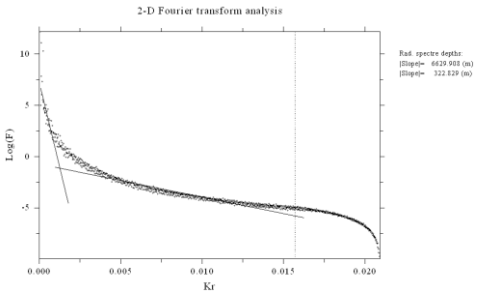

Blocks 17 & 18

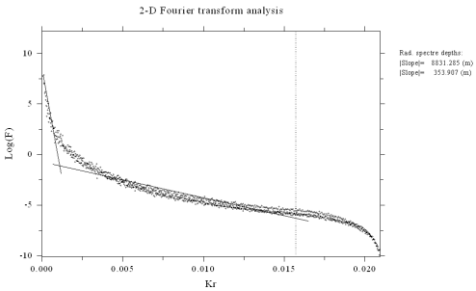

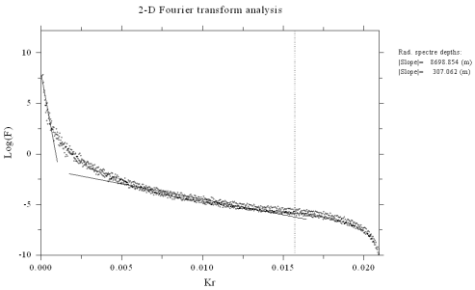

Blocks 19 & 20

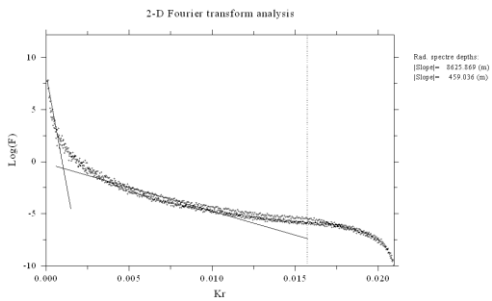

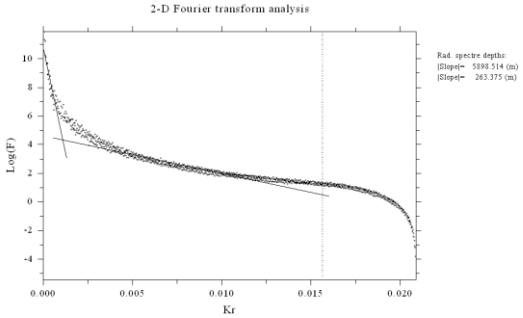

ISSN No. 2454-6194 | DOI: 10.51584/IJRIAS |Volume IX Issue IX September 2024

Blocks 21 & 22

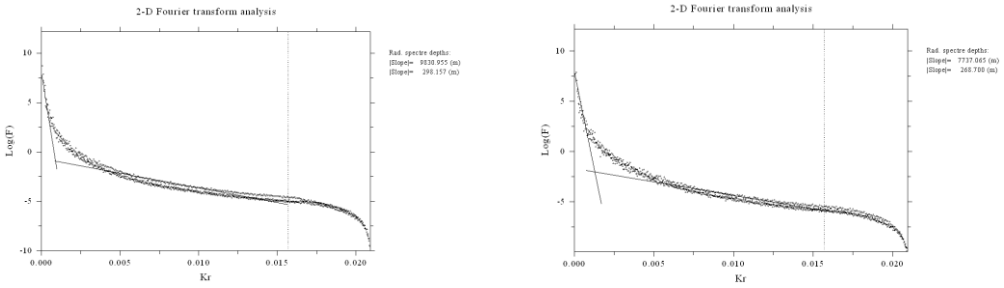

Blocks 23 & 24

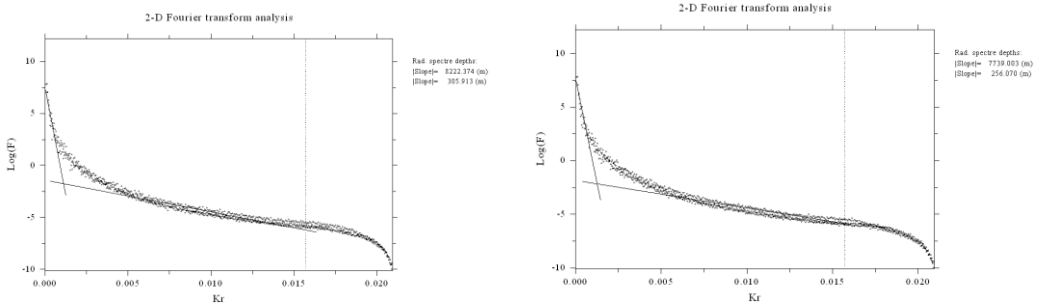

Blocks 25 & 26

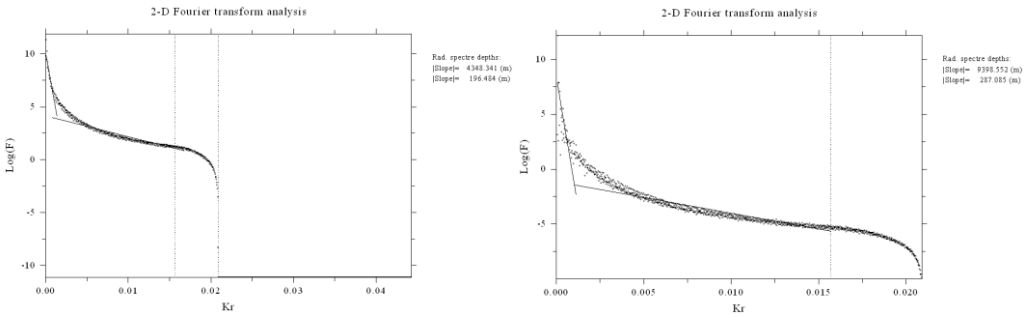

Blocks 27 & 28

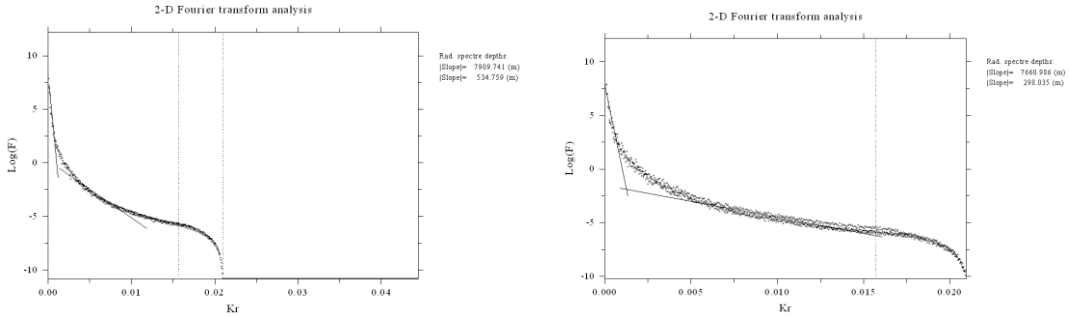

Blocks 29 & 30

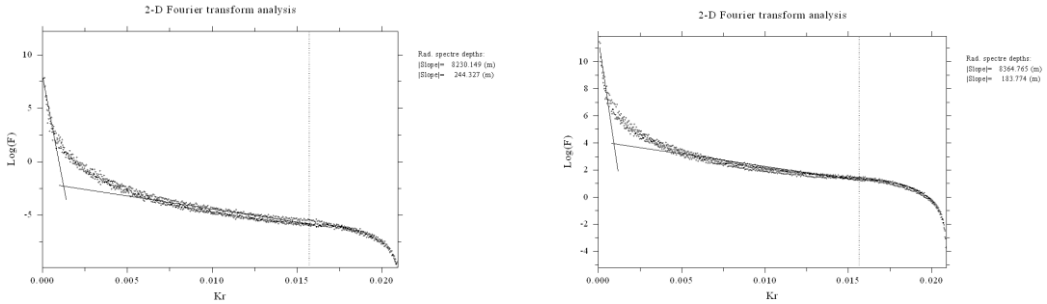

ISSN No. 2454-6194 | DOI: 10.51584/IJRIAS |Volume IX Issue IX September 2024

Blocks 31 & 32

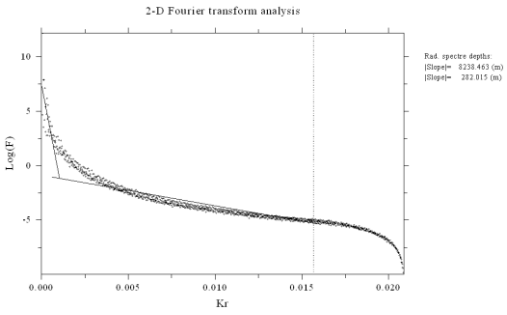

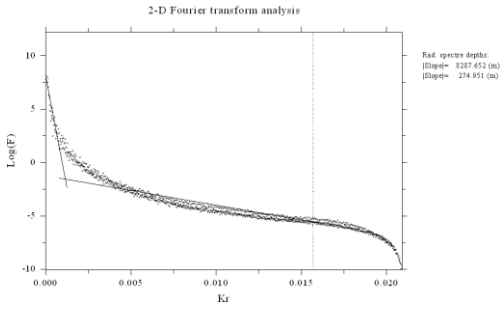

Blocks 33 & 34

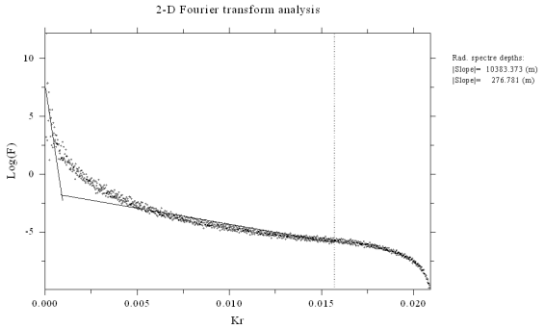

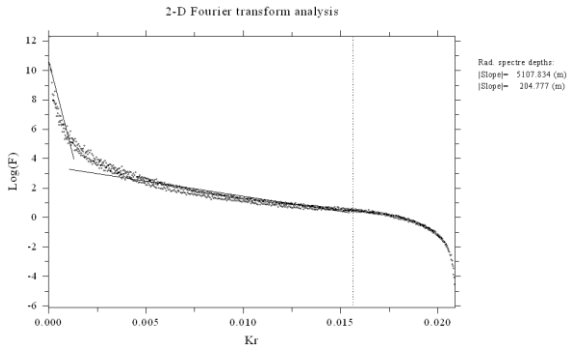

Block 35